Accepted Manuscript

Design, synthesis and biological evaluation of benzo[*cd*]indol-2(1*H*)-ones derivatives as BRD4 inhibitors

Yuxin Feng, Senhao Xiao, Yantao Chen, Hao Jiang, Na Liu, Cheng Luo, Shijie Chen, Hua Chen

PII: S0223-5234(18)30388-X

DOI: 10.1016/j.ejmech.2018.04.048

Reference: EJMECH 10397

To appear in: *European Journal of Medicinal Chemistry*

Received Date: 23 February 2018

Revised Date: 10 April 2018

Accepted Date: 23 April 2018

Please cite this article as: Y. Feng, S. Xiao, Y. Chen, H. Jiang, N. Liu, C. Luo, S. Chen, H. Chen, Design, synthesis and biological evaluation of benzo[*cd*]indol-2(1*H*)-ones derivatives as BRD4 inhibitors, *European Journal of Medicinal Chemistry* (2018), doi: 10.1016/j.ejmech.2018.04.048.

Design, Synthesis and Biological Evaluation of Benzo[*cd*]indol-2(1*H*)-ones Derivatives as BRD4 inhibitors

Yuxin Feng, Senhao Xiao , Yantao Chen, Hao Jiang, Na Liu, Cheng Luo, Shijie Chen* and Hua Chen*

A series of novel derivatives **4-9** and **11-54** bearing with benzo[*cd*]indol-2(1*H*)-one scaffold have been designed and synthesized through structure-based optimization on a lead BRD4 inhibitor **1**. Compounds **23**, **24**, **28** and **44** are the most potential BRD4 inhibitors and compounds **23** and **44** exhibit significantly inhibitory activities against MLL-rearranged MV4-11 cells proliferation.

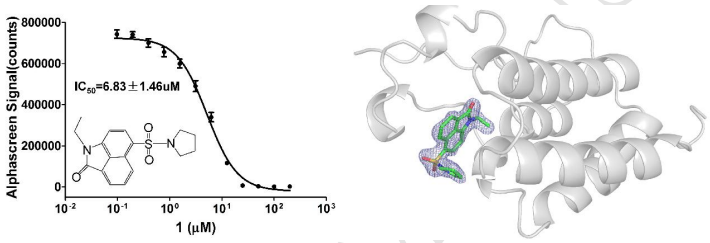

Contents lists available at ScienceDirect

European Journal of Medicinal Chemistry

journal homepage: http://www.elsevier.com/locate/ejmech

Research Paper

Design, Synthesis and Biological Evaluation of Benzo[*cd*]indol-2(1*H*)-ones Derivatives as BRD4 inhibitors

Yuxin Feng[a], Senhao Xiao[b,c,d,#], Yantao Chen[b,c], Hao Jiang[b,c], Na Liu[a], Cheng Luo[b,c], Shijie Chen[b,c*] and Hua Chen[a*]

[a]*Key Laboratory of Chemical Biology of Hebei Province, College of Chemistry and Environmental Science, Hebei University, Baoding 071002, China*

[b]*Drug Discovery and Design Center, State Key Laboratory of Drug Research, Shanghai Institute of MateriaMedica, Chinese Academy of Sciences, Shanghai 201203, China*

[c]*University of Chinese Academy of Sciences, Beijing 100049, China*

[d]*School of Life Science and Technology, Shanghai Tech University, Shanghai 200031, China*

ARTICLE INFO

Article history:

Received

Revised

Accepted

Available online

Keywords:

Benzo[*cd*]indol-2(1*H*)-one

Sulfonamide

BRD4 inhibitor

Bromodomain and extra-terminal domain

Acetyl-lysine binding pocket

ABSTRACT

Compound **1** bearing with benzo[*cd*]indol-2(1*H*)-one scaffold was identified as an effective BRD4 inhibitor through the AlphaScreen-based high-throughput screening and its high-resolution crystal structure with BRD4_BD1 protein. A series of 48 compounds were designed and synthesized by structural optimization on compound **1**. All the compounds have been evaluated for their BRD4 inhibitory activities. The results showed that compounds **23**, **24**, **28** and **44** are the most potential ones with the IC_{50} values of 1.02 μM, 1.43 μM, 1.55 μM and 3.02 μM, respectively. According to their co-crystal structures in complex with BRD4_BD1 and the protein thermal shift assays, the binding modes were revealed that the additional indirect hydrogen bonds and hydrophobic interactions make such four compounds more active than **1** against BRD4. Furthermore, compounds **1**, **23** and **44** were chosen to evaluate for their antiproliferative activities on the MLL-AF4-expression acute leukemia cell line (MV4-11), other cancer cell lines (MDA-MB-231, A549, 22Rv1) and the non-cancer cell lines (HUV-EC-C, MRC5, RPTEC). The results showed that these compounds exhibited good and selective inhibitory activities against MV4-11 cells with the IC_{50} values of 11.67 μM, 5.55 μM, and 11.54 μM, respectively, and could act on the cell proliferation by blocking cell cycle at G1 phase. They could markedly down-regulate the expressions of the c-Myc, Bcl-2 and CDK6 oncogenes in MV4-11 in the qRT-PCR and western blot studies, which further demonstrated that compound **1** and its derivatives could serve as a promising therapeutic strategy for MLL leukemia by targeting BRD4_BD1 protein.

[#]Co-first author; *Correspondence: E-mail:hua-todd@163.com; Tel & Fax.: 0086-312-5971116;

E-mail:shijiechen@simm.ac.cn; Tel & Fax.: 0086-021-50806600.

1. Introduction

Bromodomain-containing protein 4 (BRD4), belonging to the bromodomain and extra-terminal domain (BET) family of proteins, is responsible for recognizing the specific ε-*N* acetylated lysine residues on histone tails[1-3]. As the 'readers' of lysine acetylation state, BRD-containing proteins play a key role in gene transcription and epigenetics by binding acetylated lysines (KAc) on chromatin structures. These proteins have been implicated in diverse human diseases, such as cancer, diabetes, inflammation and cardiovascular diseases[4-6]. For instance, BRD4 can promote transcription of the c-MYC and Bcl-2 oncogenes, which are key regulators for the proliferation and survival of tumor cells[7-9]. Hence, BRD4 is becoming a hot target for cancer drug discovery, and its acetyl-lysine (KAc) binding pockets provide a 'druggable' site which is suitable for small molecule inhibitor development[10-12].

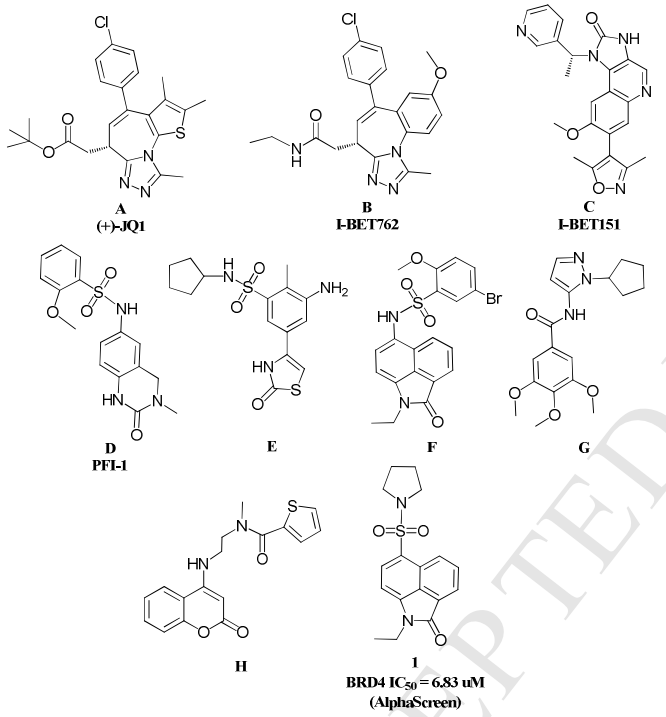

Fig. 1 The structures of BRD4 inhibitors.

Many BRD4 inhibitors with different scaffolds have been reported in the literature, such as the compounds **A-H** (Fig. 1)[13-24]. Compound **A** ((+)-JQ1) with triazolothienodiazepine was the first potent BET inhibitor with an IC_{50} value of 77 nM against BRD4 in the AlphaScreen assay[13]. Its analog I-BET762 (compound **B**) has entered clinical trials for cancer treatment[14]. Compound **C** (I-BET151) bearing with isoxazoloquinaoline was discovered in GSK through fragment-based approach and expressed in vivo efficacy against MLL-fusion leukemia[15,16]. By the application of the same approach, compounds **D** (PFI-1) and **E** were identified as the selective sulfonamide inhibitors with IC_{50} values of 220 nM and 140 nM against BRD4, respectively[17,18]. As an alternative way, structrue-based screening methods have also been widely used to find BRD4 inhibitors for different chemotypes. Compound **F**, having benzo[*cd*]indol-2(1*H*)-one acaffold[19], was described as a specific BRD4 inhibitor with significant activity, high selectivity and good pharmacokinetic profile derived from the optimization of a structrue-based screening hit[20]. Luo *et al* recently reported two series of potent inhibitors **G** and **H**, which were identified as BRD4 inhibitors through the application of high-throughput screening and crystallography[21,22]. Although there are many reported inhibitors, the discovery of novel potent inhibitors still attracts many attentions due to their therapeutic potential for various human diseases[23,24]. The diverse inhibitors will also provide pharmacological tools to investigate the fine structure and the different functions of BRD4 protein.

Generally, the small-molecule inhibitors can anchor into the KAc binding pocket of BRD4 as an acetylated lysine mimic through forming a direct hydrogen bond with the conserved asparagine 140 (N140) at the bottom of the pocket and indirect hydrogen bonds via water molecule. They are also able to interact with the WPF shelf composed of W81, P82 and F83 or the ZA channel region which constitute the active KAc binding pocket[20,25,26]. Recently, we found a new BRD4 ligand **1** (Fig. 1) bearing with benzo[*cd*]indol-2(1*H*)-one scaffold through high-throughput screening. On the basis of a good understanding the X-ray crystallograpthic support available, herein, we would like to report the optimization of the derivatives of **1** (Scheme 1) to explore its chemistry space for the potent drug discovering and the more detailed structure activity relationships (SAR) investigation. All of the new compounds were evaluated for their BRD4 inhibitory activities.

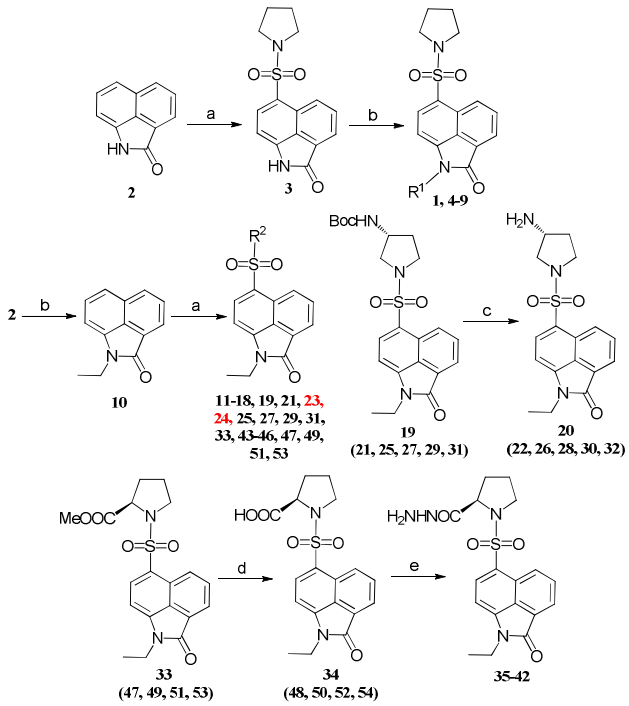

Scheme 1. The design and synthesis of compounds **1, 4-9** and **11-54**. *Conditions and reagents*: (a) 1) HSO_3Cl, $CHCl_3$, 0-50 °C; 2) Secondary amines or amino acid esters, CH_2Cl_2, DIPEA, rt., two steps: 40-80% yields; (b) Chloroalkane or bromoalkane, NaH, DMF, rt., 46-82% yields; (c) 90% CF_3COOH-H_2O, rt., 68-82% yields; (d) NaOH, MeOH, rt., 85% yields; (e)

NH_2NH_2 (or NH_2OH, aromatic amine), HATU, DIPEA, 50 °C, 38-75% yields.

2. Results and Discussions

2.1 Discovery of a potent BRD4_BD1 inhibitor.

In this study, we performed AlphaScreen based high-throughput screening[27] from our in-house library which contained 20,000 small molecules (Fig S1). The primary screening was performed with all 20,000 compounds at concentration of 100 μM. Then, we chose 37 compounds with inhibition rate higher than 90% for further validation. After two rounds of screening, 17 candidate compounds were selected for futher IC_{50} determination. The structures and inhibitory activities were shown in Table S1, which exhibited compound **1** had the best avtivity. Therefore, we identified **1** as a hit compound and subsequently determine its IC_{50} value of 6.83 ± 1.46 μM by AlphaScreen assay in three independent experiments. (Fig 2A). To confirm the scaffold authenticity of the compound **1**, and, also to delineate the bind mode for performing structure-based optimization, we determined a high resolution X-ray crystal structure of the first bromodomain of BRD4 (BRD4_BD1) in complex with compound **1** (PDB code: 5Z90). As shown in Fig 2B, the acetylated lysine binding pocket of BRD4_BD1 was occupied by compound **1** and the ligand fitted in the electron-density map well. Previous studies indicated that N140 played a crucial role in the substrates binding to BRD4_BD1[6]. The carbonyl of lactam of compound **1** did form a hydrogen-bond with N140 (Fig 2C). Besides, another indirect hydrogen-bond was formed between the carbonyl and tyrosine 97 (Y97) via a water molecule. Both the direct and indirect hydrogen-bonds contributed to the affinity of compound **1** to the protein. Moreover, compound **1** was also able to interact with the WPF shelf by means of hydrophobic interactions (Fig 2C and 2D). Except for the WPF shelf, residues (V87, L92, Y139, I146 and M149) surrounding the ligand also formed hydrophobic interactions with **1** and contributed to its activity (Fig 2D). In conclusion, the obtained crystal structure of compound **1** in complex with BRD4 was a direct and powerful proof of that compound **1** could compete with the endogenous substrate for active site binding. The structure of the complex also set up the basis for us to conduct further structure-based optimization.

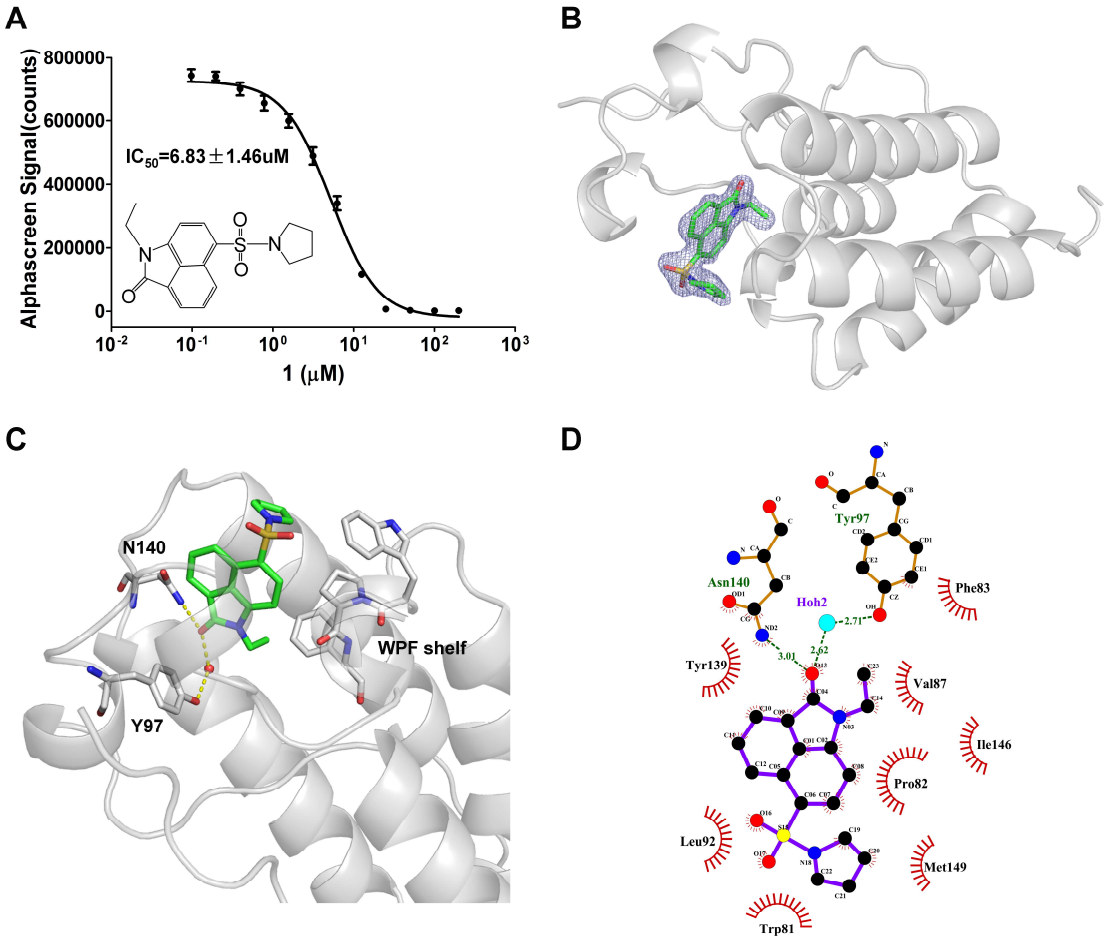

Fig 2. (A) Inhibition activity determination for compound **1** disrupting the interaction of BRD4_BD1 and peptide substrates. (B) Crystal structure of the first bromodomain of BRD4 in complex with compound **1** (PDB ID: 5Z90). (C) Molecular interactions between compound **1** and key residues of BRD4_BD1. Protein residues are shown in grey sticks with labeled names, structural waters in red spheres, respectively. Hydrogen bonds are shown as dotted yellow lines. (D) 2D diagram of interaction between compound **1** and the surrounding residues within the binding pocket of BRD4_BD1.

2.2 Chemistry

Synthesis of compound **1** and its derivatives **4-9** and **11-54** were outlined in Scheme 1. Briefly, the commercially available benzo[*cd*]indol-2(1*H*)-one **2** reacted with chlorosulfonic acid followed by pyrrolidine treatment to generate the intermediate **3**. The nucleophilic substitutions of **3** with a variety of chloroalkane or bromoalkane provided the *N*-alkyl substitution products **1** and **4-9**.

As an alternative way, compound **10** was firstly obtained by treatment with **2** and ethyl chloride. Then, compound **10** reacted with chlorosulfonic acid to give the sulfonyl chloride intermediate which was subsquently ammonolyzed with various secondary amines or amino acid esters to afford the desired sulfonamide products **11-18**, **19**, **21**, **23-25**, **27**, **29**, **31**, **33**, **43-46**, **47**, **49**, **51** and **53**.

t-Butyloxycarbonyl (Boc) group in **19**, **21**, **25**, **27**, **29** and **31** were removed in 90% CF_3COOH to achieve the products **20**, **22**, **26**, **28**, **30** and **32**, respectively.

The ester in **33**, **47**, **49**, **51** and **53** were hydrolyzed in the presence of base to afford the acid derivatives **34**, **48**, **50**, **52** and **54**, respectively. The condensation of **34** with hydrazine, or hydroxylamine or aromatic amine using tetramethyluronium hexafluorophosphate (HATU) and *N*-ethyldiisopropylamine (DIPEA) as catalysts at room temperature gave the products **35-42**.

The structures of all the newly compounds were determined by NMR, (HR) MS and element analysis. Both analytical and spectral data of compounds are in agreement with the proposed structures.

2.3. BRD4_BD1 inhibitory activity

All the newly synthesized compounds **1**, **4-9** and **11-54** were evaluated for their BRD4_BD1 inhibitory activities at the concentrations of 20 μM and 5 μM via AlphaScreen assay (Table 1 and 2). Compound **1** was used as the positive control.

Since the lactam in **1** could interact with Asn140 and the adjacent water molecule by hydrogen-bonds, we initiated the structural modification on this fragment for affinity improvement. Compounds **4-9** with various substituents attached to the lactam were designed to increase the binding interaction. However, no matter the change of the length of alky chain or the introduction of some polar groups, such as carbonyl, hydroxyl, carboxyl, or amide groups, the anti-BRD4 activities of **4-9** reduced markedly (Table 1). The results were consistent with the reported results[20], suggesting that the ethyl group attached to the lactam in compound **1** is the most favorable group to accommodate well into the acetyl lysine site of the KAc binding pocket.

Subsequently, we focused our optimization on the pyrrolidine of the sulfonamide which occupied the hydrophobic WPF shelf. The results are shown in Table 2. We preferentially evaluated some different secondary amines (**11-13**) having similar size with pyrrolidine and an aromatic amine (**14**). Compound **11** with piperidine (six-membered ring) exhibited significant BRD4 inhibitory activity at both 20 μM and 5 μM, nearly same with that of **1**, while **12** and **13** with morpholine and diethylamine, respectively, showed good activities at 20 μM. Compound **14** with the *ortho*-methoxylphenylamine had poor activity.

To further explore SAR, 3-hydroxyl and 3-/4-amino groups were incorporated into the pyrrolidine and piperidine (**15-32**), respectively. As shown in Table 2, compounds **23**, **24** and **28** with 3-hydroxyl or 3-amino on piperidine expressed very significant inhibitory activities. Overall, the activities of compounds bearing with the naked hydroxyl or amino, such as **15**, **16**, **20**, **22**, **23**, **24**, **26**, **28** and **30**, were more better than those of the corresponding ones with Boc protection group, which suggested that the hydroxyl or amino were more favorable for their inhibitory activities possibly through forming an additional hydrogen-bond as the donor. This postulation was supported by the compounds **17** and **18** with 3-methoxyl on pyrrolidine that showed poor activities. Furthermore, SAR analysis suggested that the compounds containing hydroxyl were more active than those having amino except **28**, for examples **15**, **16** versus **21**, **22**, and **23**, **24** versus **26**. Compounds **26**, **30** and **32** exhibited similar inhibition ratio, suggesting that the position of amino on piperidine seemed to have little influence on their inhibitions.

the pyrrolidine of the sulfonamide were displaced by proline and its derivatives to give compounds (**33-44**). As shown in Table 2, compound **33** with proline methyl ester exhibited similar inhibitory activity against BRD4 with that of **1** at both 20 μM and 5 μM. Compounds **34-36** with more polar groups on proline showed moderate activities, while the aromatic amide derivatives **37-42** had no activities. In this series, the reductive products **43** and **44,** in which the carboxyl was reduced to hydroxyl, showed good BRD4 inhibitory activities, especially, the later was more active than **1** at 5 μM. This observation also indicated that the hydroxyl group on the pyrrolidine and piperidine had an important role in the binging between BRD4_BD1 and the ligands.

The pyrrolidine was further changed with amino alcohol chain or amino acid (ester) to afford compounds **45-54** based on above SAR analysis. However, most of the compounds **45-54** had no or poor inhibitions possibly due to their flexibility, except **46** and **52**. Both compounds containing 3-amino-propanol and D-valine, respectively, had moderate activities against BRD4_BD1.

The compounds with the inhibition rate above that of **1** at 5 μM were chosen to further evaluate their IC_{50} values (Table 2, Fig S2). It could be seen that compounds **23**, **24**, **28** and **44** exhibited the most potential activities against BRD4_BD1 with the IC_{50} values of 1.02 ± 0.08, 1.43 ± 0.23, 1.55 ± 0.43 and 3.02 ± 1.26, respectively.

Above insights should be helpful to guide further design and synthesis of the more potent BRD4_BD1 inhibitors derived from compound **1**.

Table 1. BRD4_BD1 inhibitory activities of **1** and **4-9**.

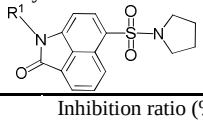

Compds.	R^1	Inhibition ratio (%)	IC_{50} (μM)

		20 μM	5 μM	(mean ± SD)
1		99	59	6.83 ± 1.46
4		25	5	N. D. [b]
5		15	-[a]	N. D.
6		9	7	N. D.
7		8	-	N. D.
8		4	-	N. D.
9		-	-	N. D.

[a]: No activity;

[b]: Not determined.

2.4. Protein Thermal shift

To confirm the binding between BRD4_BD1 protein and our compounds, we next carried out protein thermal shift assay[20]. As shown in Fig 3, compared to DMSO control, the melting temperature (Tm values) of BRD4_BD1 protein was evidently increased due to the addition of compound **1** and its derivatives at a concentration of 100 μM. The results indicated that the ligands had interaction with BRD4_BD1 protein and could strengthen its stability *in vitro*.

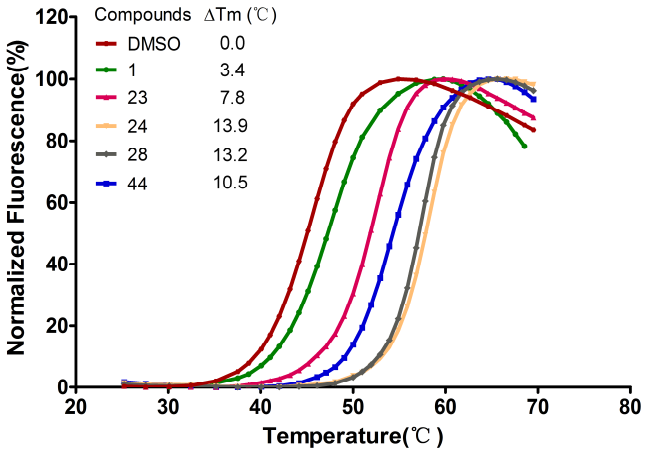

Fig 3. The melting curves of BRD4_BD1 protein with the compounds. The thermal shift assay displayed the stabilization of the BRD4_BD1 by adding compound **1** and its derivatives at a concentration ratio of 1:20 (100 μM).

2.5. Co-crystal structures of BRD4_BD1 inhibitors

In order to further explore the structure-activity relationships of compound **1** and its analogs, we determined the co-crystal structures of compound **23**, **24**, **28** and **44** in complex with BRD4-BD1, respectively. According to the structures (Fig 4), the same direct and indirect hydrogen bonds formed between N140, Y97 and compound **1**, as well as the hydrophobic interactions with the WPF shelf existed in the all four co-crystal structures. As expected, an additional indirect hydrogen bond was formed between isoleucine 146 (I146) and the hydroxyl group in **23**, **44** and the amino group in **28** via another water molecule (Fig 4A, 4C and 4D). This extra interaction further strengthened the interactions between compounds **23**, **28** and **44** and the binding site of the protein. However, because of the opposite orientation of the hydroxyl group of compound **24**, the excess hydrogen bond did not exist between the compound and I146 due to overlarge distance (Fig 4B). This may partly explain that the activity of compound **24** was slightly lower than that of compound **23**. Additionally, **24** also formed hydrophobic interactions with residues L94 and D145 except those existed in the interactions between compound **1** and protein (Fig 2B and Fig S4B), which may make it have better activity than that of **1**. In terms of compound **44**, although it formed the extra hydrogen bond, residues participated in the hydrophobic interactions were less than those of compound **23** and **28** (Fig S4A, C, D), which possibly result in its the weakest inhibitory activity among these three compounds.

Table 2. BRD4_BD1 inhibitory activities of **11-54**.

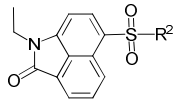

Compds.	R^2	Inhibition ratio (%)		IC_{50} (μM)	Compds.	R^2	Inhibition ratio (%)		IC_{50} (μM)
		20 μM	5 μM	(mean ± SD)			20 μM	5 μM	(mean ± SD)

11		99	58	N. D.[b]	**33**		97	55	N. D.
12		82	29	N. D.	**34**		82	33	N. D.
13		67	21	N. D.	**35**		88	35	N. D.
14		8	17	N. D.	**36**		80	28	N. D.
15		95	57	N. D.	**37**	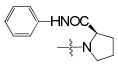	-	3	N. D.
16		88	37	N. D.	**38**	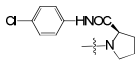	-	-	N. D.
17		27	9	N. D.	**39**	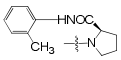	14	-	N. D.
18	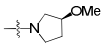	20	9	N. D.	**40**	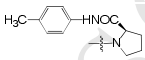	-	-	N. D.
19	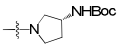	20	7	N. D.	**41**	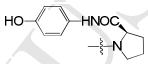	-	-	N. D.
20	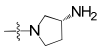	45	18	N. D.	**42**	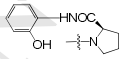	16	-	N. D.
21	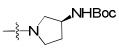	18	-[a]	N. D.	**43**		74	23	N. D.
22		61	27	N. D.	**44**		98	66	3.02 ± 1.26
23		100	93	1.02 ± 0.08	**45**		50	7	N. D.
24		100	87	1.43 ± 0.23	**46**	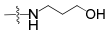	89	42	N. D.
25	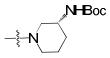	39	-	N. D.	**47**	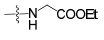	51	8	N. D.
26		63	18	N. D.	**48**	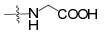	-	-	N. D.
27	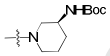	22.4	11	N. D.	**49**	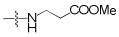	4	9	N. D.
28		100	98	1.55 ± 0.43	**50**	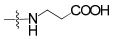	-	-	N. D.
29	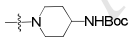	12	-	N. D.	**51**	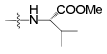	53	-	N. D.
30	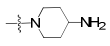	66	29	N. D.	**52**		60	41	N. D.
31		89	21	N. D.	**53**		-	-	N. D.
32		71	37	N. D.	**54**		-	4	N. D.

[a]: No activity;

[b]: Not determined.

2.6. MLL-rearranged cell activity and cell cycle analysis

As BET family was determined as a therapeutic target in acute myeloid leukemia (AML)[28], tens of inhibitors have been proceed in phase□or□clinical trial these years[29]. In this study, we used MLL-AF4-expression acute leukemia cell line (MV4-11) to perform cell-based assays. Firstly, we performed a 3-days cell viability assay against MV4-11 cell lines. Besides the parent compound **1**, **23** and **44** were chosen for cellular activity evaluation, which show the best inhibitory activity among its classification. As shown in Fig 5A, after treated with compounds **1**, **23** and **44**, reduction of viable cells was observed with an IC_{50} value of 11.67 μM, 5.55 μM, and 11.54 μM, respectively. The results showed that the compounds had effective inhibition on MV4-11 cell proliferation. In addition, we also carried the cell proliferation assays of these active compounds on the non-cancer cell lines (HUV-EC-C, MRC5, RPTEC) and other cancer cell lines (MDA-MB-231, A549, 22Rv1). As shown in Fig S5, the three compounds showed lower inhibitory activities on the non-leukemia cancer cell lines than that of MV4-11 and minimal effects on normal cell lines. The results suggested that compounds **1**, **23** and **44** have potent selectivity over other cell lines, especially the non-cancer cells lines.

To further investigate the mechanism of the anti proliferation effects, we performed cell cycle analysis and treated the MV4-11 cells with different concentrations of compounds for 24 h. The results showed these compounds could induce evidently cell cycle arrest at G1 phase in a dose-dependent manner (Fig 5B and Fig S6).

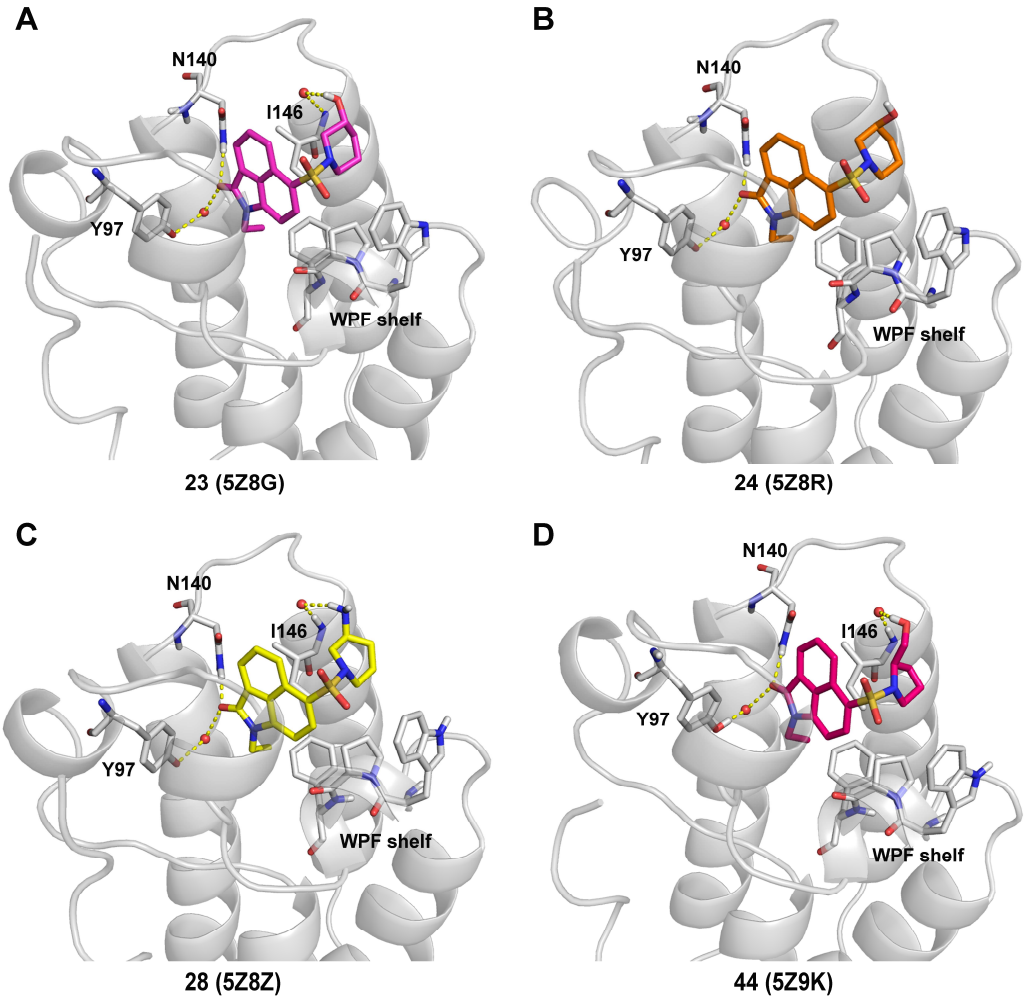

Fig 4. Co-crystal structures of compounds **23** (A), **24** (B), **28** (C), and **44** (D) with BRD4_BD1 (PDB IDs: 5Z8G, 5Z8R, 5Z8Z, and 5Z9K, respectively). The ligands are shown as sticks, and the protein is shown as a cartoon. The binding site residues are shown as sticks, structural waters are in red spheres, respectively. Hydrogen bonds interactions are indicated by dashed lines in yellow.

2.7. Down regulation of the expression of BET family target genes

The BET family plays a crucial role on the transcription of c-Myc, Bcl-2, CDK6 oncogenes, thus BRD4 inhibitors could

induce down regulation of these target genes in both transcription and translation level[30]. To further confirm the anti proliferation effect was caused by the inhibition of BRD4, we further performed real-time quantative flouresence PCR and western Blot in MV4-11 cells to detect these target genes. As shown in Fig 5C and 5D, remarkable dose-dependent decreases of target genes expression were observed at mRNA and protein level, respectively. The results demonstrated that the anti proliferation effect of our compounds was, at least in part, due to the inhibition of BRD4 in leukemia cell lines. Based on these data, compound **1** and its derivatives might serve as a promising therapeutic strategy for MLL leukemia by targeting BRD4_BD1 protein.

3. Conclusions

A series of 48 compounds have been designed and synthesized through structure-based optimization on the parent compound **1** containing benzo[*cd*]indol-2(1*H*)-one scaffold, which was authenticated as a BRD4 inhibitor through the AlphaScreen-based high-throughput screening and its high-resolution crystal structure with BRD4_BD1 protein. Among them, compounds **23**, **24**, **28** and **44** are the most potential inhibitors against BRD4 with the IC_{50} values of 1.02 μM, 1.43 μM, 1.55 μM and 3.02 μM, respectively. The co-crystal structures of the four compounds revealed that the additional indirect hydrogen bond with I146 and the hydrophobic interactions with residues L94 and D145 make such compounds more active than **1** against BRD4. Compounds **1**, **23** and **44** exhibited good and selective inhibitory activities against MV4-11 cells, and could act on the cell proliferation by blocking cell cycle at G1 phase. The direct cellular inhibition activities were found that compounds **1**, **23** and **44** also could effectively decrease the expressions of the c-Myc, Bcl-2 and CDK6 genes in MV4-11 in the qRT-PCR and western blot studies. All the results demonstrated that compound **1** and its derivatives could serve as the promising BRD4 inhibitors for MLL leukemia treatment.

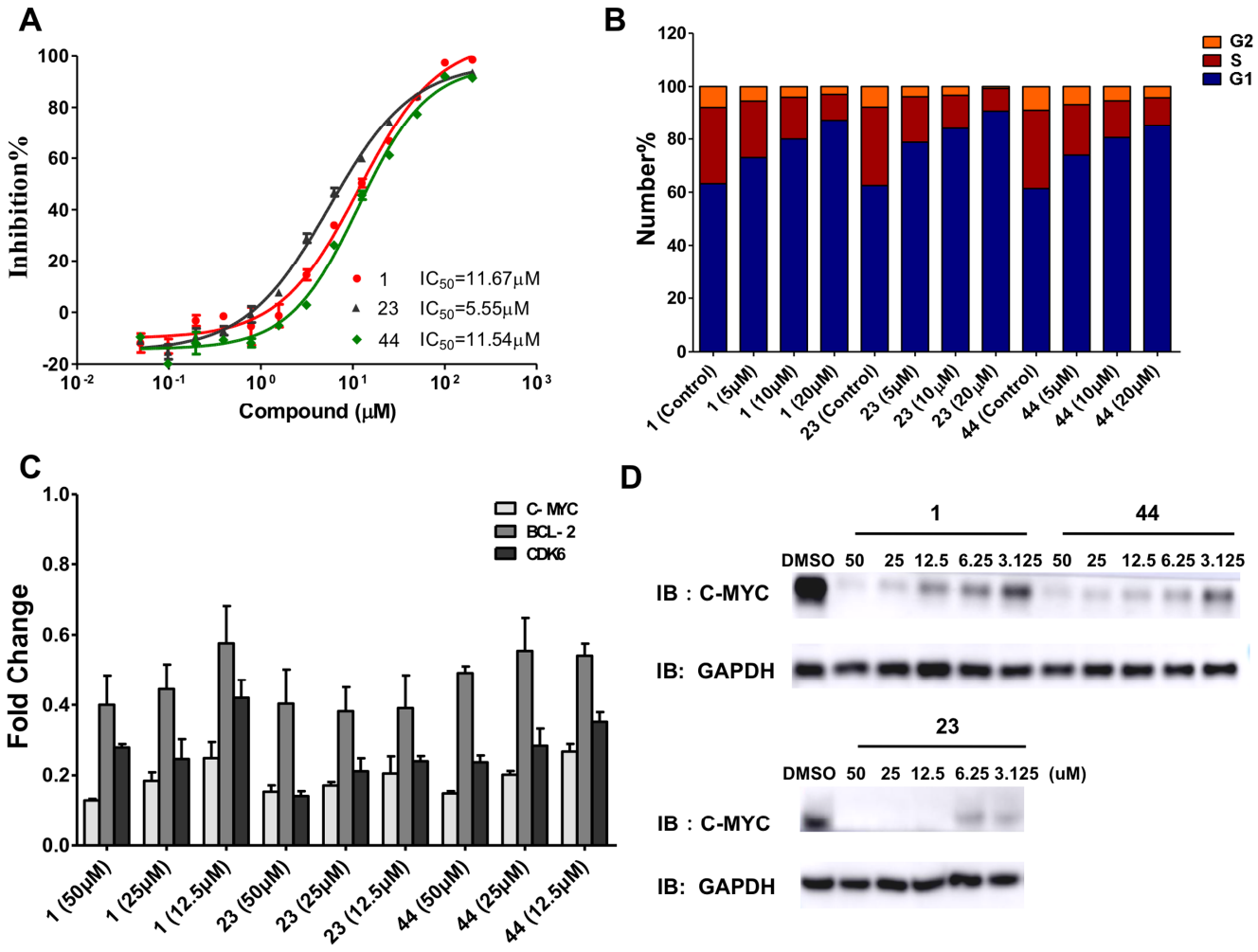

Fig 5. Cellular activities of compound **1**, **23**, and **44**. (A) Cell proliferation inhibition curves of compounds for the MV4-11 cell lines at 72 hours. (B) MV4-11 cells were arrested at G1 phase by compounds at 24 hours. (C) Quantitative RT-PCR ananlysis revealed compound **1**, **23**, and **44** could down regulate the transcription of c-Myc, Bcl-2 and CDK6 genes in MV4-11 cells after treating with them for 6 hours. (D) Treatment with compounds for 6 hours could dose-dependently decrease the protein of c-Myc in MV4-11 cells.

4. Experimental section

4.1. General

Column chromatography was carried out on flash silica gel (300-800 mesh). TLC analysis was conducted on silica gel plates (Silica G UV254). Melting points were measured in an open capillary on a SGW X-4 melting point apparatus and are uncorrected. NMR spectra were recorded at 400 MHz and 600 MHz for ^{1}H on a Bruker instrument. Chemical shifts (δ values) and coupling constants (*J* values) are given in ppm and hertz, respectively, using TMS (^{1}H NMR) solvents as internal standards. The High Resolution Mass Spectra (HRMS) were carried out on a FTICR-MS (Ionspec 7.0T) mass spectrometer with electrospray ionization (ESI). Element analysis was performed using a Heraeus (CHNO, rapid) elemental analyzer. The silica gel (300-400 mesh) for flash column chromatography was from Qingdao Marine Chemical (China).

*4.2. General procedure for the synthesis of compounds **1** and **4-9***

To a solution of benzo[*cd*]indol-2(1*H*)-one **2** (10 g, 60 mmol) in chloroform (150 mL) was added batches of chlorosulfonic acid (22 mL, 6.0 equiv.) at 0 °C for 30 min. The reaction mixture was heated at 50 °C for 5 h. The mixture was then poured into ice water and extracted with $CHCl_3$ (100 mL × 3). The organic layer was washed with brine and dried over Na_2SO_4. The solid was filtered off, and the filtrate was concentrated under reduced pressure to afford 2-oxo-1,2-dihydrobenzo[*cd*]indole-6-sulfonyl chloride (10 g, yield 50%). The resulting crude product was resolved in dichloromethane (100 mL), then the solution was added into pyrrolidine (3.4 mL, 1.2 equiv.) and *N*-ethyldi isopropylamine (DIPEA, 18 mL, 3.0 equiv.). The reaction mixture was stirred at room temperature for 5 h. After completion of the reaction as monitored by TLC, dilute HCl was added, the aqueous layer was extracted with DCM (80 mL × 3), and the organic layer was washed with water and brine, dried with Na_2SO_4, and evaporated to give 6-(pyrrolidin-1-ylsulfonyl) benzo[*cd*]indol-2(1*H*)-one **3** (9 g, yield 80%).

The product **3** (150 mg, 0.5 mmol) and sodium hydride (NaH, 36 mg, 1.5 mmol) were dissolved in DMF (15 mL). Bromoethane (65.4 mg, 0.6 mmol) was added dropwise into the solution and the reaction mixture was stirred at room temperature. After completion of the reaction as monitored by TLC, the reaction mixture was extracted with ethyl acetate (10 mL × 2). The organic layer was washed with brine and dried over Na_2SO_4. The solid was filtered off, and the filtrate was concentrated under reduced pressure. The crude product was purified by silica gel chromatography with petroleum ether/ethyl acetate (3/1, v/v) to yield compound **1**.

Under the same conditions, compounds **4-9** were obtained (for detail, see Supporting information 1 and 2).

*1-ethyl-6-(pyrrolidin-1-ylsulfonyl)benzo[cd]indol-2(1H)-one (**1**):*

Yellow-green solid, yield 77%, m.p. 168.1-168.9 °C; ^{1}H NMR (600 MHz, $CDCl_3$) δ (ppm): 8.79 (d, *J* = 8.4 Hz, 1H), 8.16 (d, *J* = 7.2 Hz, 1H), 8.11 (d, *J* = 7.2 Hz, 1H), 7.83 (t, *J* = 7.8 Hz, 1H), 6.96 (d, *J* = 7.8 Hz, 1H), 3.99 (q, *J* = 7.2 Hz, 2H), 3.31 (t, *J* = 6.6 Hz, 4H), 1.79 - 1.77 (m, 4H), 1.39 (t, *J* = 7.2 Hz, 3H); ^{13}C NMR (150 MHz, $CDCl_3$) δ (ppm): 167.6 (C=O), 143.6, 132.9 (CH), 130.4 (CH), 130.3 (CH), 127.0, 126.5, 125.8 (2C), 125.2 (CH), 103.0 (CH), 47.5 ($2CH_2$), 35.1(CH_2), 25.3 ($2CH_2$), 13.9 (CH_3); HRMS (ESI): Calcd for $C_{17}H_{18}N_2O_3SNa$ ($[M+Na]^+$): 353.0936, Found: 353.0932. Anal. Calcd for $C_{17}H_{18}N_2O_3S$: C, 61.80; H, 5.49; N, 8.48. Found: C, 61.78; H, 5.52; N, 8.49.

*4.3. General procedure for the synthesis of compounds **11-18**, **19**, **21**, **23**, **24**, **25**, **27**, **29**, **31**, **33**, **43-46**, **47**, **49**, **51** and **53***

Following the above synthetic procedure of **1** from **3**, the *N*-ethyl intermediate **10** (9 g, yield 80%) were obtained using **2** (10 g, 60 mmol) as the starting material. The sulfonamide compound **11** was prepared by the ammonolysis reactions of the corresponding sulfonyl chloride subsititution with piperidine according to the above procedure from **2** to **3**.

Under the same conditions, compounds **12-18**, **19**, **21**, **23**, **24**, **25**, **27**, **29**, **31**, **33**, **43-46**, **47**, **49**, **51** and **53** were obtained (for detail, see Supporting information 1 and 2).

1-ethyl-6-(piperidin-1-ylsulfonyl)benzo[cd]indol-2(1H)-one (**11**):

Yellow-green solid, yield 78%, m.p. 126.2 - 126.7 °C; ^{1}H NMR (600 MHz, $CDCl_3$) δ (ppm): 8.70 (d, *J* = 8.4 Hz, 1H), 8.08 (d, *J* = 7.2 Hz, 1H), 8.07 (d, *J* = 7.2 Hz, 1H), 7.80 (t, *J* = 7.8 Hz, 1H), 6.95 (d, *J* = 7.8 Hz, 1H), 3.97 (q, *J* = 7.2 Hz, 2H), 3.07 (t, *J* = 5.4 Hz, 4H), 1.61 - 1.58 (m, 4H), 1.40 - 1.36 (m, 5H); ^{13}C NMR (150 MHz, $CDCl_3$) δ (ppm): 167.5 (C=O), 143.7, 133.4 (CH), 130.4 (CH), 130.3 (CH), 126.5, 126.1, 125.7, 125.6, 125.2 (CH), 103.1 (CH), 46.5 ($2CH_2$), 35.1 (CH_2), 25.2 ($2CH_2$), 23.4 (CH_2), 13.9 (CH_3); HRMS (ESI): Calcd for $C_{18}H_{20}N_2O_3SNa$ ($[M+Na]^+$): 367.1092, Found: 367.1090. Anal. Calcd for $C_{18}H_{20}N_2O_3S$: C, 62.77; H, 5.85; N, 8.13. Found: C, 62.75; H, 5.88; N, 8.16.

*4.4. General procedure for the synthesis of compounds **20**, **22**, **26**, **28**, **30** and **32***

Compound **19** (100 mg, 0.2 mmol) was dissolved in 2 mL DCM and 2 mL 90% CF_3COOH. The mixture was stirred at room temperature. After completion of the reaction as monitored by TLC, solid $NaHCO_3$ was added to the solution to neutralize the acid, and the solution extracted with water (3 mL) and ethyl acetate (12 mL). The organic solvent was in sequence washed with the distilled water (10 mL × 4), the saturated brine (10 mL × 2), dried with $MgSO_4$ for 5 h, then evaporated under vacuum to afford the crude product. The residue was purified by silica gel chromatography with dichloromethane/methanol (15/1, v/v) to afford the compound **20**.

Under the same conditions, compounds **22**, **26**, **28**, **30** and **32** were obtained (for detail, see Supporting information 1 and 2).

*(R)-6-((3-aminopyrrolidin-1-yl)sulfonyl)-1-ethylbenzo[cd]indol-2(1H)-one (**20**):*

Yellow-green solid, yield 80%, m.p.161.0 - 162.1 °C; ^{1}H NMR (600 MHz, CD_3OD) δ (ppm): 8.75 (d, *J* = 8.4 Hz, 1H), 8.17 (d, *J* = 7.8 Hz, 1H), 8.08 (d, *J* = 7.0 Hz, 1H), 7.90 (t, *J* = 7.8 Hz, 1H),

7.24 (d, *J* = 7.2 Hz, 1H), 3.99 (q, *J* = 7.2 Hz, 2H), 3.71 - 3.68 (m, 1H), 3.54 - 3.52 (m, 1H), 3.45 (dd, *J* = 10.8, 6.6 Hz, 1H), 3.30 (d, *J* = 5.4 Hz, 1H), 3.27 - 3.22 (m, 1H), 2.20 - 2.14 (m, 1H), 1.87 - 1.82 (m, 1H), 1.35 (t, *J* = 7.2 Hz, 3H); ^{13}C NMR (150 MHz, CD_3OD) δ (ppm): 169.2 (C=O), 145.2, 135.1 (CH), 131.8 (CH), 131.4 (CH), 127.6, 126.9, 126.8, 126.7, 126.4 (CH), 105.3 (CH), 53.1 (CH), 51.2 (CH_2), 46.9 (CH_2), 36.1 (CH_2), 31.4 (CH_2), 14.1 (CH_3); HRMS (ESI): Calcd for $C_{17}H_{19}N_3O_3SNa$ ($[M+Na]^+$): 368.1045, Found: 368.1041. Anal. Calcd for $C_{17}H_{19}N_3O_3S$; C, 59.11; H, 5.54; N, 12.17. Found: C, 59.12; H, 5.56; N, 12.14.

*4.5. General procedure for the synthesis of compounds **34**, **48**, **50**, **52** and **54***

To a solution of **33** (300 mg, 0.8 mmol) in 25 mL methanol was added NaOH (93mg, 2.4mmol). The reaction mixture was stirred at 50 °C. After completion of the reaction as monitored by TLC, 12N HCl was added to the solution to neutralize the base. The solvent was removed under reduced pressure. The residue was purified by silica gel chromatography with dichloromethane/ methanol (3/1, v/v) to afford the compound **34**.

Under the same conditions, compounds **48**, **50**, **52** and **54** were obtained (for detail, see Supporting information 1 and 2).

*1-((1-ethyl-2-oxo-1,2-dihydrobenzo[cd]indol-6-yl)sulfonyl)pyrrolidine-2-carboxylic acid (**34**):*

Yellow solid, yield 85%, m.p. 199.5 - 200.7 °C; ^{1}H NMR (600 MHz, CD_3OD) δ (ppm): 8.81 (d, *J* = 8.4 Hz, 1H), 8.21 (d, *J* = 7.8 Hz, 1H), 8.09 (d, *J* = 7.2 Hz, 1H), 7.89 (t, *J* = 7.8 Hz, 1H), 7.22 (d, *J* = 7.8 Hz, 1H), 4.28 (brs, 1H), 4.00 (q, *J* = 7.2 Hz, 2H), 3.53 (d, *J* = 6.6 Hz, 1H), 3.36 (brs, 1H), 1.97 - 1.92 (m, 3H), 1.67 - 1.65 (m, 1H), 1.36 (t, *J* = 7.2 Hz, 3H); ^{13}C NMR (150 MHz, CD_3OD) δ (ppm): 180.0 (C=O), 169.4 (C=O), 144.5, 134.4 (CH), 132.2 (CH), 131.5 (CH), 129.4, 127.4, 126.9, 126.7, 126.2 (CH), 105.4 (CH), 64.4 (CH), 49.9 (CH_2), 36.1 (CH_2), 32.7 (CH_2), 25.8 (CH_2), 14.1 (CH_3); HRMS (ESI): Calcd for $C_{18}H_{18}N_2O_5SNa$ ($[M+Na]^+$): 397.0834, Found: 397.0832. Anal. Calcd for $C_{18}H_{18}N_2O_5S$: C, 57.74; H, 4.85; N, 7.48. Found: C, 57.79; H, 4.82; N, 7.51.

*4.6. General procedure for the synthesis of compounds **35-42***

To a solution of **34** (15 mg, 0.4 mmol), HATU (213 mg, 0.7 mmol) and hydrazine (16 mg, 0.5 mmol) in dry DMF (15 mL) was added DIPEA (0.21 mL, 1.2 mmol). The mixture was added for stirring at room temperature until the completion of reaction (followed by TLC).The mixture was neutralized with 0.5N HCl solution, then the residue was extracted with ethyl acetate (10 mL × 3). The organic layer was then sequentially washed with water, brine, and dried over anhydrous Na_2SO_4, evaporated to dryness under reduced pressure. The residue was purified by silica gel chromatography with dichloromethane/methanol (10/1, v/v) to afford the compound **35**.

Under the same conditions, compounds **36-42** were obtained (for detail, see Supporting information 1 and 2).

*1-((1-ethyl-2-oxo-1,2-dihydrobenzo[cd]indol-6-yl)sulfonyl)pyrrolidine-2-carbohydrazide (**35**):*

Yellow-green oil, yield 68%; ^{1}H NMR (600 MHz, $CDCl_3$) δ (ppm): 8.76 (d, *J* = 8.4 Hz, 1H), 8.15 (d, *J* = 7.8 Hz, 1H), 8.09 (d, *J* = 6.6 Hz, 1H), 7.83 (t, *J* = 7.8 Hz, 1H), 6.96 (d, *J* = 7.2 Hz, 1H), 4.25 (dd, *J* = 8.4, 2.4 Hz, 1H), 3.96 (q, *J* = 7.2 Hz, 2H), 3.60 - 3.57 (m, 1H), 3.25 - 3.21 (m, 1H), 2.11- 2.08 (m, 1H), 1.81 - 1.74 (m, 1H), 1.62 - 1.55 (m, 2H), 1.36 (t, *J* = 7.2 Hz, 3H); ^{13}C NMR (150 MHz, $CDCl_3$) δ (ppm): 171.6 (C=O), 167.4 (C=O), 144.4, 134.0 (CH), 131.0 (CH), 130.0 (CH), 126.5, 125.7 (2C), 125.6 (CH), 125.0, 103.2 (CH), 61.3 (CH), 49.3 (CH_2), 35.1 (CH_2), 30.4 (CH_2), 24.4 (CH_2), 13.8 (CH_3); HRMS (ESI): Calcd for $C_{18}H_{20}N_4O_4SNa$ ($[M+Na]^+$): 411.1103, Found: 411.1108. Anal. Calcd for $C_{18}H_{20}N_4O_4S$: C, 55.66; H, 5.19; N, 14.42. Found: C, 55.69; H, 5.15; N, 14.46.

4.7 Protein purification

His-tagged BRD4_BD1 construct was cloned into a modified pET28a vector and expressed in the *E. Coli* strain BL21(DE3). Cells were grown at 37 °C until OD600 reach a value of 0.6, induced with 0.4 mM IPTG and incubated overnight at 16 °C. The protein was initially purified by Ni-NTA affinity chromatography, and followed by an anion exchange chromatography without cleave the 6x His-Tag. The protein was further purified using a Superdex 75 (10/300) column (GE Healthcare) equilibrated with a buffer containing 20 mM HEPES (pH 7.4), 100 mM NaCl and 1 mM DTT. The protein was concentrated and flash-frozen in liquid nitrogen and stored at -80 °C.

4.8 Crystallization

For crystallization, the 6x His-Tag need to be removed by TEV protease at 4 °C overnight. The protein was further purified by size exclusion chromatography (GE Healthcare) in a buffer containing 10 mM HEPES (pH 7.4), 100 mM NaCl and 5 mM DTT. The peak fraction was collected and concentrated to 7 mg/mL for crystallization. Crystals were obtained in a crystallization reagent (4 M sodium formate and 15% glycerol) at 16 °C by sitting-drop vapour-diffusion method. The crystals were soaked in the crystallization reagents plus compounds and 1% DMSO for 4 or 5 days. The X-ray diffraction data of the small molecule and BRD4_BD1 complex was collected at Shanghai Synchrotron Radiaton Facilities (SSFR), BL19U. The data was analyzed as previously described[31].

4.9 AlphaScreen assay

The amplified luminescent proximity homogeneous assay (AlphaScreen) was performed as previously described[31]. In general, the acceptor and donor beads were purchased at Perkin Elmer. The sequence of biotin-labelled substrate peptide was SGRG-K(Ac)-GG-K(Ac)-GLG-K(Ac)-GGA-K(Ac)-RHRKVGG-K-Biotin (synthesized by Shanghai China Peptide Corporation, purity > 95%). The assay was performed in an

assay buffer containing 20 mM HEPES, pH 7.4, 0.1% bovine serum albumin (w/v), 0.01% Triton X-100 and 1 mM DTT at a volume of 20 μL. The BRD4_BD1 protein need to be incubated with compounds at room temperature first. After 15 min, biotin-labelled peptide was added into the plate (OptiPlate-384, PerkinElmer) for 10 min. Then the streptavidin donor beads and nickel chelate acceptor beads were added and incubated for 60 min. The signal counts were then measured by EnVision (PerkinElmer) and analyzed by Graphpad Prism 5.0.

4.10 Protein thermal shift

The thermal shift assay was performed in an assay buffer containing 20 mM HEPES, pH 7.4, 100 mM NaCl, 1 mM DTT. The reaction system contained 5×SYPRO® Orange dye (Invitrogen, 5000×stock in DMSO), 5 μM Brd4_BD1 protein plus 0.5% DMSO or 100 μM compounds to make the final DMSO concentration equal. The melting curve was generated by heating the plate with a slope of 2.5 °C/min from 25 °C to 95 °C. The assay was performed on QuantStudioTM 6 Flex real-time PCR machine (Applied Biosystems) and analyzed by the software Protein Thermal Shift™v1.3 (Applied Biosystems).

4.11 Cell Proliferation assay

MV4-11 cells were obtained from the American Type Culture Collection and cultured in RPMI 1640 medium supplemented with 10% FBS (Life Technologies) and 1% penicillin/ streptomycin (Life Technologies). For the cell proliferation assay, MV4-11 cells were plated in 96-well plates at a density of 1×10^5 /mL in a volume of 100 μL. About one hour later, different concentrations of diluted compounds or DMSO control were added into the plates in a volume of 25 μL and incubateted for 72 h. Normal cell lines HUV-EC-C (normal vascular endothelium cells), MRC5 (normal lung fibroblast cells), RPTEC (normal kidney epithelial cells) and cancer cell lines A549 (non-small cell lung cancer cells), MDA-MB-231 (triple negative breast cancer cells), 22Rv1 (prostate cancer cells) were also obtained from the American Type Culture Collection and plated in 96-well plates at a density of 3×10^4 /mL in a volume of 100 μL. The cell viability was determined by CellTiter-Glo Luminescent Cell Viability Assay (Promega) as the manufacture insturcted. The luminescence was measured by EnVision (Perkin Elmer). Every dilution point was run in triplicate, the data of which was averaged and analyzed in Graphpad Prism 5.0.

4.12 Cell cycle analysis

For the cell cycle analysis, MV4-11 cells were cultured in 6 well plates at the density of 5×10^5/mL at a volume of 2 mL. The cells were treated with 20 uM, 10 uM, 5 uM compounds or DMSO control for 24h. Then the cells were harvested and resuspended in PBS which containing 70% ethanol for fixation at 4 °C overnight. Then, the cells were washed by PBS to remove the ethanol and stained by PI/Rnase Staining Buffer (BD pharmingen) for 15 min. The sample was immediately measured and analyzed by BD FACSCalibur (BD Pharmingen).

4.13 Quantitative real time PCR

MV4-11 cells were cultured in 6 well plates at the density of 5×10^5/mL. Different concentrations of compounds or DMSO control were added into the plates and incubateted for 6 hours. The cells were then harvested and washed by PBS twice. The total RNA was extracted by TRIzol Reagent kit (Vazyme Viotech) and immediately performed reverse transcription using HiScript II Q RT SuperMix Kit (Vazyme Biotech). Then, the qRT-PCR assay was performed on the Quant Studio 6 Flex Real-Time PCR system (Applied Biosystems) using SYBR Green Real-Time PCR Master Mix (VazymeViotech). The data was analysized by the $\Delta\Delta Ct = \Delta Ct\ (GENE\text{-}B2M)_{normal} - \Delta Ct\ (GENE\text{-}B2M)_{cancer}$ method.

4.14 Western Blot

MV4-11 cells were plated in six wells plate at the density of 5×10^5/mL at a volume of 2 mL. The cells were treated with different concentrations of compounds or DMSO control for 6 hours. The primer antibodies (c-Myc, CST) were diluted in a ratio of 1:1000 and incubated at 4 °C overnight. Then, the secondary antibodies were diluted in a ratio of 1:10000 (Anti-Rabbit, CST) and incubated for 1 h at room temperature. Imaging was performed on ChemiScope3400 imaging system (Amersham).

Acknowledgments

We thank the staffs from BL19U1 beam line of National Facility for Protein Science Shanghai (NFPS) at Shanghai Synchrotron Radiation Facility, for assistance during data collection. This work is supported by the National Natural Science Foundation of China (81703415 to S.C., 21472208 and 81625022 to C.L.). This work is also sponsored by Shanghai Sailing Program (17YF1423100 to S.C.).

References

[1] P. Filippakopoulos, S. Knapp, Targeting bromodomains: epigenetic readers of lysine acetylation, Nat. Rev. Drug Discovery 13 (2014) 337-356.

[2] L. Zeng, M.M. Zhou, Bromodomain: an acetyl-lysine binding domain, FEBS Lett. 513 (2002) 124-128.

[3] S.Y. Wu, C.M. Chiang, The double bromodomain-containing chromatin adaptor BRD4 and transcriptional regulation, J. Biol. Chem. 282 (2007) 13141-13145.

[4] A.C. Belkina, G.V. Denis, BET domain coregulators in obesity, inflammation and cancer, Nat. Rev. Cancer 12 (2012) 465-477.

[5] S. Muller, P. Filippakopoulos, S. Knapp, Bromodomains as therapeutic targets, Expert Rev. Mol. Med. 13 (2011) e29/1-e29/21.

[6] P. Filippakopoulos, S. Picaud, M. Mangos, T. Keates, J.P. Lambert, D. Barsyte-Lovejoy, I. Felletar, R. Volkmer, S. Muller, T. Pawson, A.C. Gingras, C.H. Arrowsmith, S. Knapp, Histone recognition and large-

scale structural analysis of the human bromodomain family, Cell 149 (2012) 214-231.

[7] J.E. Delmore, G.C. Issa, M.E. Lemieux, P.B. Rahl, J.W. Shi, H.M. Jacobs, E. Kastritis, T. Gilpatrick, R.M. Paranal, J. Qi, M. Chesi, A.C. Schinzel, M.R. McKeown, T.P. Heffernan, C.R. Vakoc, P.L. Bergsagel, I.M. Ghobrial, P.G. Richardson, R.A. Young, W.C. Hahn, K.C.Anderson, A.L. Kung, J.E. Bradner, C.S. Mitsiades, BET bromodomain inhibition as a therapeteuic strategy to target c-Myc, Cell 146 (2011) 904-917.

[8] A. Wyce, G. Ganji, K.N. Smitheman, C.W. Chung, S. Korenchuk, Y. Bai, O. Barbash, B. Le, P.D. Craggs, M.T. McCabe, K.M. Kennedy-Wilson, L.V. Sanchez, R.L. Gosmini, N. Parr, C.F. McHugh, D. Dhanak, R.K. Prinjha, K.R. Auger, P.J. Tummino, BET inhibition silences expression of MYCN and BCL2 and induces cytotoxicity in neuroblastoma tumor models, PLos One 8 (2013) e72967.

[9] J.P. Hu, Y.Q. Wang, Y.L. Li, L. Xu, D.Y. Cao, S.S. Song, M.S. Damaneh, X. Wang, T. Meng, Y.L. Chen, J.K. Shen, Z.H. Miao, B. Xiong, Discovery of a series of dihydroquinoxalin-2(1H)-ones as selective BET inhibitors from a dual PLK1-BRD4 inhibitor, Eur. J. Med. Chem. 137 (2017) 176-195.

[10] P. Brennan, P. Filippakopoulos, S. Knapp, The therapeutic potential of acetyl-lysine and methyl-lysine effector domains, Drug Discovery Today: Ther. Strategies 9 (2012), e101-e110.

[11] D.S. Hewings, T.P.C. Rooney, L.E. Jennings, D.A. Hay, C.J. Schofield, P.E. Brennan, S. Knapp, S.J. Conway, Progress in the development and application of small molecule inhibitors of bromodomain-acetyl-lysine interactions, J. Med. Chem. 55 (2012), 9393-9413.

[12] D. Gallenkamp, K.A. Gelato, B. Haendler, H. Weinmann, Bromodomains and their pharmacological inhibitors, ChemMedChem 9 (2014) 438-464.

[13] P. Filippakopoulos, J. Qi, S. Picaud, Y. Shen, W.B. Smith, O. Fedorov, E.M. Morse, T. Keates, T.T. Hickman, I. Felletar, M. Philpott, S. Munro, M.R. McKeown, Y. Wang, A.L. Christie, N. West, M.J. Cameron, B. Schwartz, T.D. Heightman,; N. LaThangue,; C.A. French, O. Wiest, A.L. Kung, S. Knapp, J.E. Bradner, Selective inhibition of BET bromodomains, Nature 468 (2010) 1067-1073.

[14] O. Mirguet, R. Gosmini, J. Toum, C.A. Clément, M. Barnathan, J.M. Brusq, J.E. Mordaunt, R.M. Grimes, M. Crowe, O. Pineau, M. Ajakane, A. Daugan, P. Jeffrey, L. Cutler, A.C. Haynes, N.N. Smithers, C.W. Chung, P. Bamborough, I.J. Uings, A. Lewis, J. Witherington, N. Parr, R.K. Prinjha, E. Nicodème, Discovery of epigenetic regulator I-BET762: Lead optimization to afford a clinical candidate inhibitor of the BET bromodomains, J. Med. Chem. 56 (2013) 7501-7515.

[15] O. Mirguet, Y. Lamotte, F. Donche, J. Toum, F. Gellibert, A. Bouillot, R. Gosmini, V.L. Nguyen, D. Delannee, J. Seal, F. Blandel, A.B. Boullay, E. Boursier, S. Martin, J.M. Brusq, G. Krysa, A. Riou, R. Tellier, A. Costaz, P. Huet, Y. Dudit, L. Trottet, J. Kirilovsky, E. Nicodème, From ApoA1 upregulation to BET family bromodomain inhibition: discovery of I-BET151, Bioorg. Med. Chem. Lett. 22 (2012) 2963-2967.

[16] J. Seal, Y. Lamotte, F. Donche, A. Bouillot, O. Mirguet, F. Gellibert, E. Nicodeme, G. Krysa, J. Kirilovsky, S. Beinke, S. McCleary, I. Rioja, P. Bamborough, C.W. Chung, L. Gordon, T. Lewis, A.L. Walker, L. Cutler, D. Lugo, D.M. Wilson, J. Witherington, K. Lee, R.K. Prinjha, Identification of a novel series of BET family bromodomain inhibitors: binding mode and profile of I-BET151 (GSK1210151A), Bioorg. Med. Chem. Lett. 22 (2012) 2968-2972.

[17] S. Picaud, D. Da Costa, A. Thanasopoulou, P. Filippakopoulos, P.V. Fish, M. Philpott, O. Fedorov, P. Brennan, M.E. Bunnage, D.R. Owen, J.E. Bradner, P. Taniere, B. O'Sullivan, S. Muller, J. Schwaller, T. Stankovic, S. Knapp, PFI-1, a highly selective protein interaction inhibitor, targeting BET Bromodomains, Cancer Res. 73 (2013) 3336-3346.

[18] L. Zhao, D. Cao, T. Chen, Y. Wang, Z. Miao, Y. Xu, W. Chen, X. Wang, Y. Li, Z. Du, B. Xiong, J. Li, C. Xu, N. Zhang, J. He, J. Shen, Fragment-based drug discovery of 2-thiazolidinones as inhibitors of the histone reader BRD4 bromodomain, J. Med. Chem. 56 (2013) 3833-3851.

[19] J. Nie, D.D. Dong, Y. Zhang, T.Y. Wang, W. Liu, S.Z. Yi, Synthesis and biological evaluation of a benz[*cd*]indol-2(1*H*)-one derivatives, Asian J. Chem. 26 (2014) 7329-7336.

[20] X.Q. Xue, Y. Zhang, Z.X. Liu, M. Song, Y.L. Xing, Q.P. Xiang, Z. Wang, Z.C. Tu, Y.L. Zhou, K. Ding, Y. Xu, Discovery of benzo[cd]indol-2(1*H*)-ones as potent and specific BET bromodomain inhibitors: structure-based virtual screening, optimization, and biological evaluation, J. Med. Chem. 59 (2016) 1565-1579.

[21] Z.Y. Sun, H. Zhang, Z.F. Chen, Y.Q. Xie, H. Jiang, L.M. Chen, H. Ding, Y.Y. Zhang, H.L. Jiang, M.Y. Zheng, C. Luo, Discovery of novel BRD4 inhibitors by high-throughput screening, crystallography, and cell-based assays, Bioorg. Med. Chem. Lett. 27 (2017) 2003-2009.

[22] Z.F. Chen, H. Zhang, S.E. Liu, Y.Q. Xie, H. Jiang, W.H. Lu, H. Xu, L.Y. Yue, Y.Y. Zhang, H. Ding, M.Y. Zheng, K.Q. Yu, K.X. Chen, H.L. Jiang, C. Luo, Discovery of novel trimethoxy-ring BRD4 bromodomain inhibitors : ALPHAscreening, crystallography and cell-based assay, Med. Chem. Commun. 8 (2017) 1322-1331.

[23] L. Ouyang, L. Zhang, J. Liu, L.L. Fu, D.H. Yao, Y.Q. Zhao, S.Y. Zhang, G. Wang, G. He, B. Liu, Discovery of a small-molecule bromodomain-containing protein 4 (BRD4) inhibitor that induces AMP-activated protein kinase-modulated autophagy-associated cell death in breast cancer, J. Med. Chem. 60 (2017) 9990-10012.

[24] M. Zengerle, K.-H. Chan, A. Ciulli, Selective small molecule induced degradation of the BET bromodomain protein BRD4, ACS Chem. Biol. 10 (2015) 1770-1777.

[25] L.R. Vidler, N. Brown, S. Knapp, S. Hoelder, Druggability analysis and structural classification of bromodomain acetyl-lysine binding sites, J. Med. Chem. 55 (2012) 7346-7359.

[26] Z.M. Zhang, S.H. Hou, H.L. Chen, T. Ran, F. Jiang, Y.Y. Bian, D.W. Zhang,Y.L. Zhi, L. Wang, L. Zhang, H.M. Li, Y.M. Zhang, W.F. Tang, T. Lu, Y.D. Chen, Targeting epigenetic reader and eraser: Rational design, synthesis and in vitro evaluation of dimethylisoxazoles derivatives as BRD4/HDAC dual inhibitors, Bioorg. Med. Chem. Lett. 26 (2016) 2931-2935.

[27] Xiong, J. Han, J. Wang , W.C. Lu, C. Wang, Y. Chen, F.L. Lian, N.X. Zhang, Y.C. Liu, C.H. Zhang, H. Ding, H.L. Jiang, W.C. Lu, C. Luo, B. Zhou, Discovery of 1,8-acridinedione derivatives as novel GCN5 inhibitors via high throughput screening. Eur. J. Med. Chem. (2018) https://doi.org/10.1016/j.ejmech.2018.02.005.

[28] J. Zuber, J. Shi, E. Wang, A.R. Rappaport, H. Herrmann, E.A. Sison, D. Magoon, J. Qi, K. Blatt, M. Wunderlich, M.J. Taylor, C. Johns, A. Chicas, J.C. Mulloy, S.C. Kogan, P. Brown, P. Valent, J.E. Bradner, S.W. Lowe, C.R. Vakoc, RNAi screen identifies BRD4 as a therapeutic target in acute myleoid leukaemia, Nature 478 (2011) 524-528.

[29] D.B. Doroshow, J.P. Eder, P.M. LoRusso, BET inhibitors: a novel epigenetic approach, Ann. Oncol. 28 (2017) 1776-1787.

[30] M.A. Dawson, R.K. Prinjha, A. Dittmann, G. Giotopoulos, M. Bantscheff, W.I. Chan, S.C. Robson, C.W. Chung, C. Hopf, M.M. Savitski, C. Huthmacher, E. Gudgin, D. Lugo, S. Beinke, T.D. Chapman, E.J. Roberts, P.E. Soden, K.R. Auger, O. Mirguet, K. Doehner, R. Delwel, A.K. Burnett, P. Jeffrey, G. Drewes, K. Lee, B.J. Huntly, T. Kouzarides, Inhibition of BET recruitment to chromatin as an effective treatment for MLL-fusion leukaemia, Nature 478 (2011) 529-533.

[31] H. Jiang, J. Xing, C. Wang, H. Zhang, L. Yue, X. Wan, W. Chen, H. Ding, Y. Xie, H. Tao, Z. Chen, H. Jiang, K. Chen, S. Chen, M. Zheng, Y. Zhang, C. Luo, Discovery of novel BET inhibitors by drug purposing of nitroxoline and its analogues, Org. Biomol. Chem. 15 (2017) 9352-9361.

Highlights

> Compound **1** bearing with benzo[*cd*]indol-2(1*H*)-one scaffold was identified as an effective BRD4 inhibitor.

> Novel derivatives **4-9** and **11-54** were designed and synthesized by structural optimization on compound **1**.

> Compounds **23**, **24**, **28** and **44** are the most BRD4 inhibitors.

> The co-crystal structures of the inhibitors in complex with BRD4_BD1 revealed the binding mode.

> Compounds **1**, **23** and **44** inhibit MV4-11 cells proliferation by blocking cell cycle at G1 phase.

> Compounds **1**, **23** and **44** could decrease the expressions of the c-Myc, Bcl-2 and CDK6 genes in MV4-11.